

Electrochemical Analysis of Ordered Mesoporous Carbons with Discriminating Pore Structure by Removing the Template with KOH or HF

Xiaoling Zhai^{1,2}, Junqing Liu^{1,2}, Peng Li^{1,2}, Ming Zhong^{1,2}, Chang Ma^{1,2}, Huiqi Wang^{1,2},
Quangui Guo¹, Yan Song^{1,*}, Linjie Zhi^{1,3*}

¹ Key Laboratory of Carbon Materials, Institute of Coal Chemistry, Chinese Academy of Sciences, Taiyuan 030001, PR China

² Graduate University of Chinese Academy of Sciences, Beijing 100039, PR China

³ National Center for Nanoscience and Technology, Beijing, 100049, China

*E-mail: yansong1026@126.com; zhilj@nanoctr.cn

Received: 3 July 2012 / Accepted: 19 July 2012 / Published: 1 August 2012

Ordered mesoporous carbon (OMC) were prepared via template approach using phenolic resol as the carbon source, triblock copolymer as the organic precursor and tetraethyl orthosilicate (TEOS) as the template. The OMC with different pore structures were obtained by removing the silicon template with HF and KOH. Their physical structures and electrochemical properties were investigated by nitrogen adsorption-desorption, transmission electron microscope and electrochemical measurements. The results showed that the OMC prepared by removing the template with HF (OMC_{-HF}) possessed higher specific surface area (1844 m²/g) and larger pore diameter (2.5nm) than OMC by removing the template with KOH (OMC_{-KOH}). The OMC_{-HF} exhibited better electrochemical performances than OMC_{-KOH} when used as the electrode materials in electrochemical double-layer capacitors (EDLCs). The OMC_{-HF} showed higher specific capacitance (154 F/g) than OMC_{-KOH} (76F/g) at current density up to 20A/g in 6 M KOH electrolyte, owing to its high specific surface area and optimized pore structure. The excellent capacitance performance made it as favorable electrode materials in EDLCs for fast charge/discharge at high current density.

Keywords: Ordered mesoporous carbon; Pore structure; Specific capacitance; Electrochemical properties

1. INTRODUCTION

Ordered mesoporous carbon (OMC) have been attracting much attention because of their high surface area, large pore volume, chemical inertness and high mechanical stability which prompts them

show potential applications in many fields [1-3], since the first discovery of ordered mesoporous materials by Mobil scientist [4] in 1992. Electrochemical double-layer capacitors (EDLCs) are one of the most important energy sources for portable electronic devices, cold-starting assistants, electric vehicles and so on [5, 6]. OMC used as electrode materials of EDLCs due to their high power density and long cycle life [7-9] have been reported by many researchers.

Various methods are adopted to prepare OMC, including physical and chemical activation [10], carbonization of organic polymer [11], carbonization of blend polymer [12] and soft and hard template [13, 14] methods. Hard template method shows obvious advantages such as simple process and good reproducibility and so on. The hard template method was widely used to prepare OMC. While, the pore structure of OMC prepared by hard template method shows great differences related to specific synthesis conditions. The pore structure of OMC may critically affect their electrochemical properties serving as electrode materials involving the electrolyte accessibility, ion diffusion, electron conductivity, etc. [15]. Such as the impacts of pores arrangement (prepared by changing the ratio of reactants) on the specific capacitance of the OMC have been discussed by many research teams [16, 17]. Nevertheless, little attention has been focused on the process of removing the silicon template. Hydrofluoric acid and concentrated alkali are always used to remove the silicon template. It is believed that acid and alkali have different effects on the pore structure of OMC due to their disparate reactions. Therefore, more work should be done to understand the influence of removing the template by acid and alkali on the OMC.

Herein, OMC with different pore structure have been prepared via template approach by removing the silicon template with HF and KOH. The obtained OMC as electrode materials for EDLCs have been measured by electrochemical techniques. The differences in pore structure and its effect on electrochemical performance have been studied in detail.

2. EXPERIMENTAL

2.1. Preparation of OMC

First, for the synthesis of phenolic resin precursor, 2.13 g (0.023 mol) phenol was melted at 40-45 °C and mixed with 0.63 g of 20 wt % sodium hydroxide (NaOH) aqueous solution under magnetic stirring for 10 min. Then, 2.0 mL formalin (37 wt % formaldehyde) was added to the solution. After stirring for 1 h at 72-76 °C, The mixed solution was cooled down. The pH was adjusted to about 7.0 with, and the water in this mixture was removed by vacuum distillation below 50 °C. Then, the resin was dissolved in ethanol (20 wt%).

Then, the synthesis of OMC by tri-constituent co-assembly. 1.62 g of amphiphilic triblock copolymer ($\text{PO}_{97}\text{EO}_{186}\text{PO}_{97}$) was dissolved in 10.0mL ethanol with 0.3 mL of 0.6 M HCl stirring for 1 h at 35 °C. Then 2.05 g of tetraethyl orthosilicate (TEOS) and 4.08 g phenolic resol precursor (20 wt%) were added to the mixture for 2-3 h continuous stirring and then transferred to a glass dish at room temperature for 8-12 h to evaporate the ethanol and then at 100 °C for 24 h to thermopolymerize. The prepared polymer film was carbonized at 900 °C for 2-3 h under N_2 flow. Then the carbon-silica

composites were then immersed into 6M KOH and 20 wt% HF solution, respectively, to remove the silica, and the obtained samples denoted as OMC-KOH and OMC-HF, respectively.

2.2. Characterizations of OMC

Nitrogen adsorption-desorption measurements was conducted using an automatic adsorption system (ASAP2020, Micromeritics) by physical adsorption of N₂ at 77 K. Before the measurements of the sorption isotherms, the samples were degassed at 200 °C in vacuum for 6 h. Transmission electron microscopy (TEM, F30 and Hitechi H-800 operated at 200 kV). For the TEM measurements, samples were crushed in an agate mortar, dispersed in ethanol, and deposited on a microgrid.

2.3. Electrochemical measurement

For making a working electrode, the OMC (80 wt.%) was ground with 10 wt.% polytetrafluoroethylene (PTFE) and 10 wt.% acetylene black. The mixture was pressed on nickel foam to fabricate the electrodes. Hg/HgO electrode was used as reference electrode and 6 M KOH solution as the electrolyte. The counter-electrode was platinum foil. Electrochemical measurements of the samples were performed on a CHI 660C instrument (Shanghai Chenhua, China) using a three-electrode system. All the electrochemical tests were performed at room temperature.

3. RESULTS AND DISCUSSION

3.1. Pore structural analysis of OMC

Table 1. Structure parameters of the samples

Sample	S_{BET} (m ² /g)	V_{total} (cm ³ /g)	V_{mes} (cm ³ /g)	D_p (nm)
OMC-KOH	1657	1.16	1.10	2.80
OMC-HF	1844	1.63	1.59	3.53

S_{BET} – specific surface area; V_{total} - total pore volume, measured at $P/P_0 = 0.995$; V_{mes} - mesopore volume, obtained by BJH method; D_p - average pore diameter, calculated by $4V/A$ from BET

The surface area, pore volume and average pore diameter of the samples from Brunauer-Emmett-Teller (BET) are shown in Table 1. It can be found that the surface area and pore volume of OMC-HF is larger than that of OMC-KOH. Moreover, the average pore diameter of OMC-HF has obvious increase than that of OMC-KOH. The corresponding pore size distributions are shown in Fig. 1. The measured results reveal that the pore size distributions of OMC-KOH and OMC-HF calculated from the absorption branches by the Barrentt-Joyner-Halenda method are centered at 2.1 and 2.5 nm, respectively. The exact reason for this difference is not clear yet. It is probably related to the reaction

between HF and certain oxygen groups, as the loss of oxygen in the carbon framework will generate more defects in the wall of holes. There is a tendency for the pore diameter to expand by removing the template with HF. Therefore, the obtained OMC-HF has larger pore diameter.

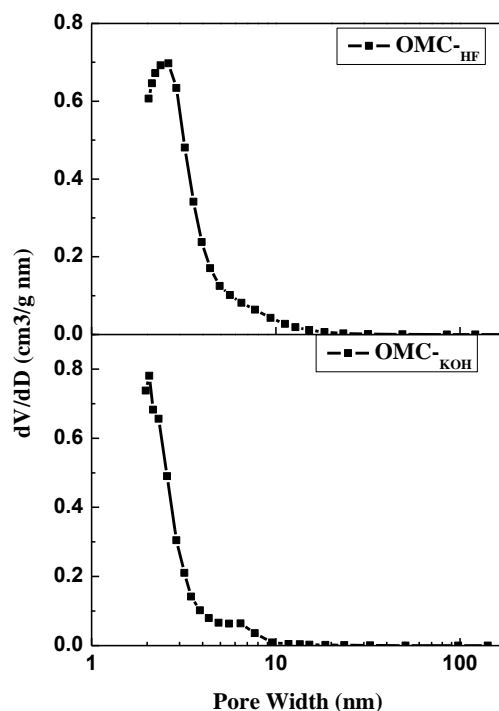


Figure 1. BJH pore size distribution of the samples

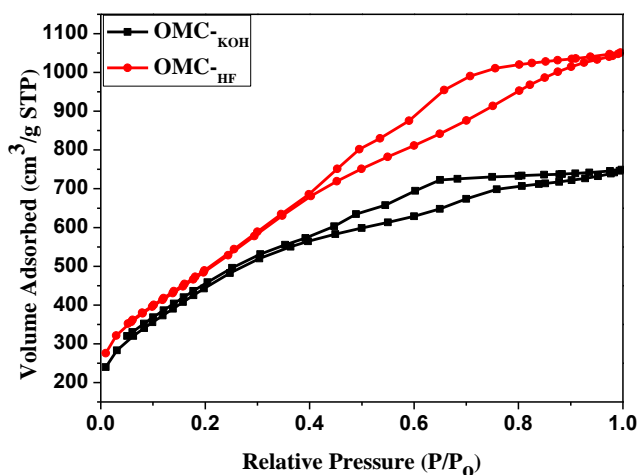


Figure 2. N2 adsorption/desorption isotherms of the samples

Fig. 2 shows the nitrogen adsorption/desorption isotherms of the samples. Both samples have the typical IV type isotherms, indicating that the samples are mesoporous materials [18]. The distinct capillary condensation steps at high relative pressures are assigned to the narrow pore size distribution

of the OMC. The measured results reveal that both samples contain abundant mesopores, which is in agreement with the results of BJH pore size distribution.

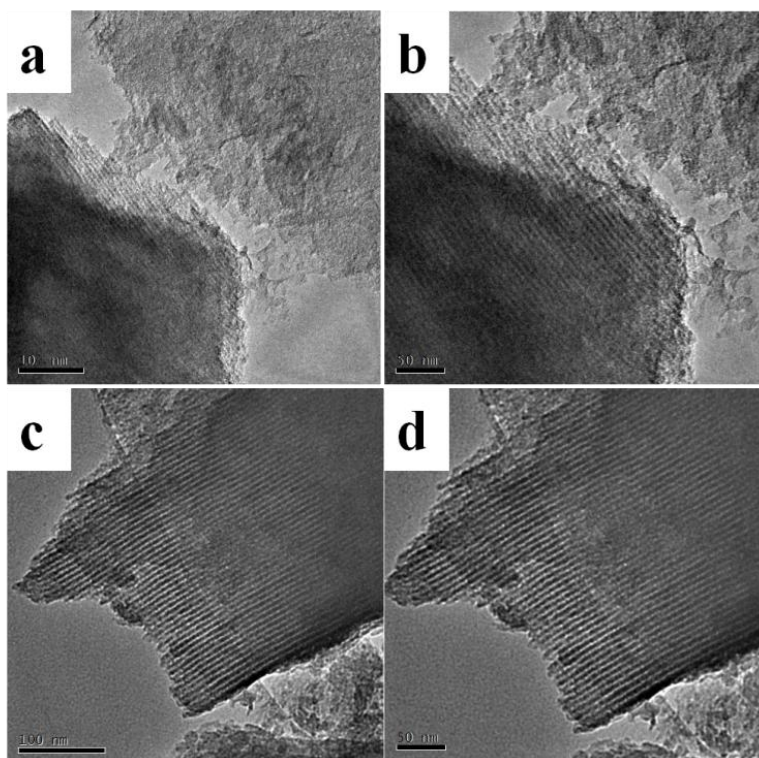


Figure 3. TEM images of the samples. a, b for OMC-KOH, c, d for OMC-HF, respectively

The microstructures of the samples are examined by TEM. Fig. 3 shows a typical TEM image of ordered pore structure viewed along [100] direction [19]. It can be observed that the samples OMC-KOH and OMC-HF have long-ordered stripe-like pore structure. The pore sizes, measured in TEM images, are also consistent with those calculated by BJH method using N₂-adsorption branches. This pore structure is beneficial to the charge transportation, which is required for EDLCs.

3.2. Electrochemical properties of OMC

To examine the electrochemical performance of the OMC, the calculated capacitances (from galvanostatic charge/discharge test) of the samples as a function of the current density are illustrated in Fig. 4. The specific capacitance (F/g) is calculated according to the formula as follows:

$$C = (i \times \Delta t) / m \Delta v$$

Where i is the discharge current in ampere, Δt is the discharge time in second, Δv is the voltage window in volt and m is the quality of active material in gram. The calculations are per single electrode of the obtained materials.

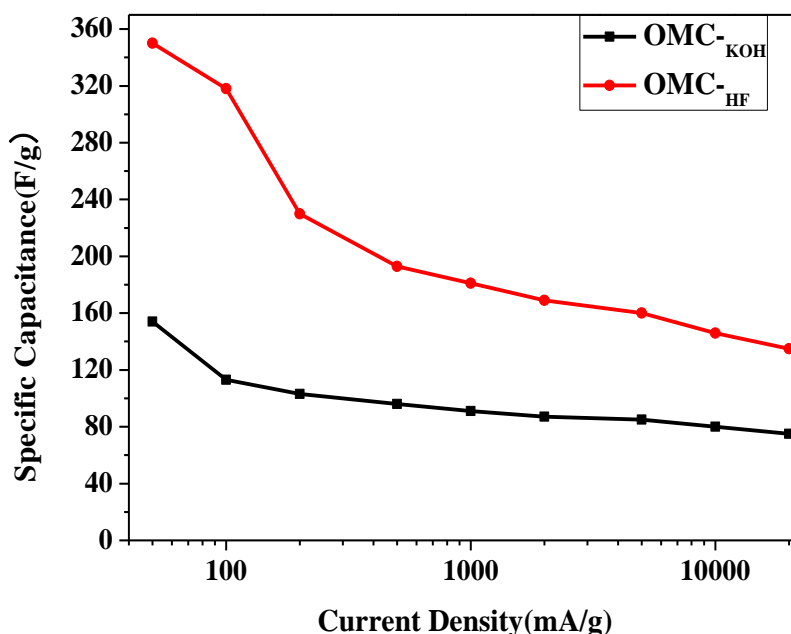


Figure 4. The specific capacitances of the samples as a function of discharging current density.

It can be seen that the values of the specific capacitance for the OMC-KOH and OMC-HF electrodes are strongly dependent on the current density from Fig. 4. In detail, the specific capacitance decreases with the increase of the current density. The reason is that the electrode and electrolyte could not form electric double layer effectively because of the faster charging and discharging at high current density.

Up to high current density of 20A/g, nearly 48 and 38% of the initial value is remained for the OMC-KOH and OMC-HF, respectively. Although the capacitance retention of OMC-HF is slightly lower than that of OMC-KOH, the specific capacitance of OMC-HF at 20 A/g is 154 F/g, which is still much higher than that of OMC-KOH (76 F/g) at the same current density. It shows that the OMC-HF electrodes allow rapid ion diffusion and exhibit good electrochemical utilization. The higher specific capacitance of OMC-HF is attributed to the larger specific surface area and optimized pore structure than that of OMC-KOH.

Fig. 5a shows the charge/discharge curves of OMC-KOH and OMC-HF electrodes at 0.5A/g. Both curves show a typical triangle symmetrical distribution, indicating a good double layer capacitive property. The discharge time of OMC-HF is much larger than that of OMC-KOH, therefore the OMC-HF exhibits larger specific capacitance than OMC-KOH at the same current density. There is a sharper voltage drop (IR) for OMC-KOH than that of OMC-HF, indicating that the mesopores in OMC-HF sample can improve the ion transfer and may reduce the inner resistance of the electrodes. The voltage drop is associated with the equivalent series resistance (ESR) of the EDLCs [20].

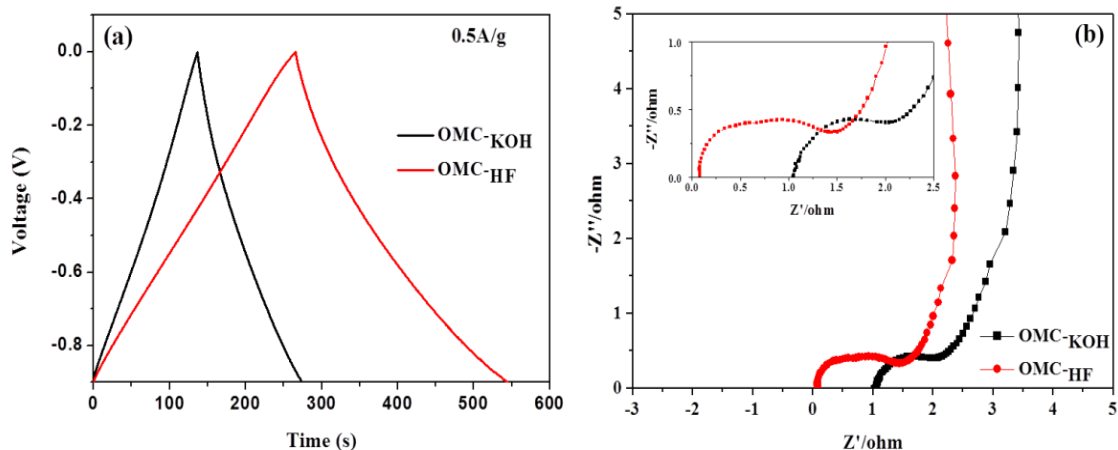


Figure 5. (a) The charge-discharge curves of OMC-KOH and OMC-HF electrodes at the current density of 0.5 A/g; (b) Nyquist plot for OMC-KOH and OMC-HF electrodes.

To further investigate the ESR, the Nyquist plots of the samples are shown in Fig. 5b. The ESR is the sum of the charge-transfer resistance of the electrode (R_{ct}) [21] and internal resistance (R_s), which includes the resistance of the electrolyte solution, the intrinsic resistance of the active material and the contact resistance at the interface of active material/current collector [22]. The semicircle diameter in the high frequency region is attributed to R_{ct} and the high frequency intercept with the real axis is related to R_s . The ESR of OMC-HF is less than that of OMC-KOH from Fig. 5b. The lower resistance of the OMC-HF sample makes it possible for higher specific capacitance.

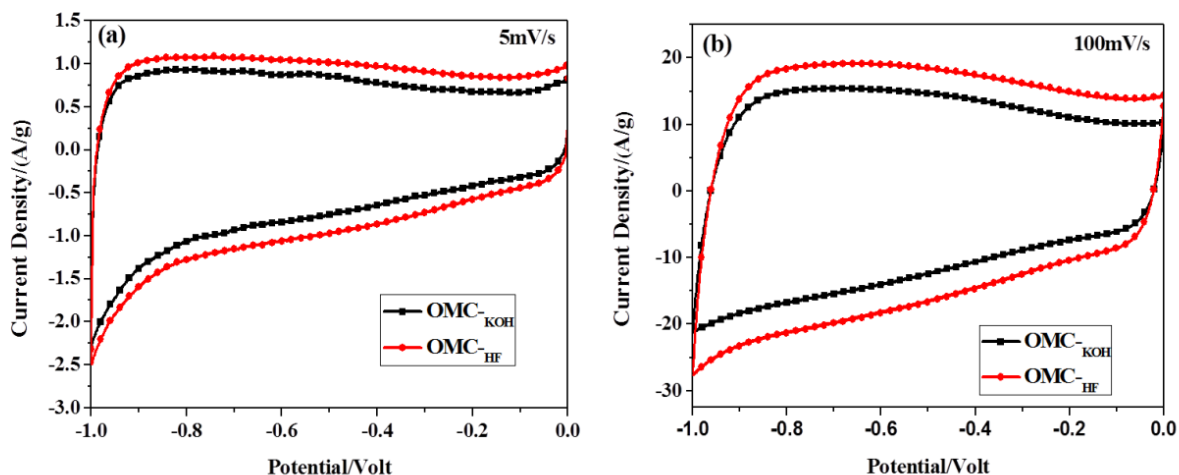


Figure 6. Cyclic voltammetry of OMC-KOH and OMC-HF electrodes measured at (a) 5 and (b) 100 mV/s

Moreover, the linear part of the sloped line represents the resistance of electrolyte ion diffusion into mesopore channels. An ideal capacitor should exhibit a vertical line. The deviation from the

vertical line is ascribed to the diffusion resistance for electrolyte ions, strongly depending on the detailed mesoporous structure [23]. The bigger slope of OMC-HF indicates its better capacitive behavior.

Fig. 6 shows the cyclic voltammetry (CV) plots of the samples at the sweep rate of 5 and 100mV/s with the potential range of -1 to 0 V vs. Hg/HgO reference electrode. At a low scan rate of 5 mV/s, both samples present near rectangular shapes with slightly distorted, indicating typically EDLC performances. It is clear that the OMC-HF electrode exhibits a larger CV area than the OMC-KOH electrode, indicating a higher specific capacitance compared with OMC-KOH. The CV curves can still maintain quasi-rectangular shapes as the sweep rate increases to 100mV/s, suggesting a highly reversible process for fast charging and discharging. In the meantime, Fig. 6a and 6b reveal that the electrochemical performance of OMC-HF is better than that of OMC-KOH, as evidenced by the still vertical slope of the current near vertex potential at high sweep rate. These results indicate the rapid ion diffusion of electrolytes in the mesopores of OMC-HF during the double-layer formation and also demonstrate that the resistance for electrolyte motion is small, assistant with the results of impedance analysis. In a word, the OMC-HF exhibits excellent capacitance performance because of high specific surface area and favorable pore structure.

4. CONCLUSIONS

OMC have been prepared via triblock copolymer, TEOS and phenolic resin tri-constituent co-assembly approach. There are differences in pore structures by using acid and alkali to remove the silicon template for the OMC. The obtained OMC-HF possesses higher specific surface area and larger pore diameter than OMC-KOH while maintaining the well ordered pore structure. The OMC-HF exhibits better electrochemical performances than OMC-KOH when used as the electrode materials in EDLCs. The OMC-HF shows higher specific capacitance (154 F/g) than OMC-KOH (76F/g) at current density up to 20A/g. Meanwhile, quasi-rectangular shapes at the sweep rate of 100mV/s and lower resistance of the OMC-HF, demonstrating its capability of fast ion diffusion within its mesoporous structure. The optimized pore structure of the OMC-HF makes it as suitable electrode materials in EDLCs for fast charge/discharge at high current density.

ACKNOWLEDGEMENTS

The research was supported by the financial support of the Natural Science Foundation of China (50602046, 20973044, 21173057), the Ministry of Science and Technology of China (2012CB933403), the ICC CAS Fund for distinguished Young Scientist, the State Education Ministry, and the Natural Science Foundation of Shanxi Province (NO.2012011019-3)

References

1. T. Shunsuke, N. Norikazu, E. Yasuyuki, U. Korekazu, *Chem. Commun.*, 41 (2005) 2125
2. S. Yoon, J.W. Lee, T. Hyeon, S.M. Oh, *J. Electrochem. Soc.*, 147 (2000) 2507

3. P. Li, Y. Song, Y. Geng, M. Zhong, Q. Guo, J.L. Shi, L. Liu, *Int. J. Electrochem. Sci.*, 7 (2012) 4039
4. C.T. Cresge, M.E. Leonowicz, W.J. Roth, J.C. Vartuli, J.S. Beck, *Nature.*, 359 (1992) 701
5. M. Winter, R.J. Brodd, *Chem. Rev.*, 104 (2004) 4245
6. W. R. Li, D. H. Chen, Z. Li, Y. F. Shi, Y. Wan, J. J. Huang, J. J. Yang, D. Y. Zhao, and Z. Y. Jiang, *Electrochem. Commun.*, 9 (2007) 569
7. J. Lee, S. Yoon, T. Hyeon, S.M. Oh, K.B. Kim, *Chem. Commun.*, 21 (1999) 2177
8. I. Moriguchi, Y. Koga, R. Matsukura, Y. Teraoka, M. Kodama, *Chem. Commun.*, 24 (2002) 1844
9. J. Lee, S. Yoon, S.M. Oh, C.H. Shin, T. Hyeon, *Adv. Mater.*, 12 (2000) 359
10. E. Ruckenstein, H.H. Yun, *Carbon*, 36 (1998) 269.
11. S. Gavaldà, K. Kaneko, K.T. Thomson, K.E. Gubbins, *Colloids Surf., A*, 1872 (2001) 531
12. J. Ozaki, N. Endo, W. Ohizumi, K. Igarashi, M. Nakahara, *Carbon*, 35 (1997) 1031
13. R. Ryoo, S.H. Joo, S. Jun, *J. Phys. Chem. B*, 103 (1999) 7743
14. S. Tanaka, N. Nishiyama, Y. Egashira, K. Ueyama, *Chem. Commun.*, 2005(17) 2125
15. H.J. Liu, X.M. Wang, W.J. Cui, Y.Q. Dou, D.Y. Zhao, Y.Y. Xia, *J. Mater. Chem.*, 20 (2010) 4223
16. J. Zhang, L.B. Kong, J.J. Cai, H. Li, Y.C. Luo, L. Kang, *Micropor. Mesopor. Mater.*, 132 (2010) 154
17. J.W. Lang, X.B. Yan, X.Y. Yuan, J. Yang, Q.J. Xue, *J. Power Sources*, 196 (2011) 10472
18. S. Jun, S. H. Joo, R. Ryoo, M. Kruk, M. Jaroniec, Z. Liu, T. Ohsuna, O. Terasaki, *J. Am. Chem. Soc.*, 122 (2000) 10712
19. Y. Meng, D. Gu, F.Q. Zhang, Y.F. Shi, H.F. Yang, Z. Li, C.Z. Yu, B. Tu, D.Y. Zhao, *Angew. Chem.*, 117 (2005) 7215
20. H.L. Guo, Q.M. Gao, *J. Power Sources*, 186 (2009) 551
21. F. Xu, G.D. Zheng, D.C. Wu, Y.R. Liang, Z.H. Li, R.W. Fu, *Phys. Chem. Chem. Phys.*, 12 (2010) 3270.
22. S.R. Sivakkumar, W.J. Kim, J.A. Choi, D.R. MacFarlane, M. Forsyth, D.W. Kim, *J. Power Sources*, 171 (2007) 1062
23. D.S. Yuan, J.H. Zeng, J.X. Chen, Y.L. Liu, *Int. J. Electrochem. Sci.*, 4 (2009) 562